Development of a Module for Fire Dynamics

A Major Qualifying Project Report

Submitted to the Faculty of

WORCESTER POLYTECHNIC INSTITUTE

in partial fulfillment of the requirements for the

Degree of Bachelor of Science

Submitted by: Alana Miska

Report Submitted to: Professor James Urban

Worcester Polytechnic Institute (WPI)

April 27th, 2023

This report represents the work of one or more WPI undergraduate students submitted to the faculty as evidence of completion of a degree requirement. WPI routinely publishes these reports on the web without editorial or peer review.

Acknowledgements

Many thanks to everyone who supported and provided guidance for the completion of this project. First and foremost, thanks to my advisor, Professor Urban, for his notable advice and counsel throughout the project, as well as for providing me with this project opportunity. Thanks to Frederick Brokaw, UL Fire Protection Engineering Performance Lab Manager, for all his advice and assistance to successfully conduct fire experiments. I would also like to thank Jorge Valdivia and Fernando Ebensperger for providing Python code to retrieve weight scale data from the laboratory load cells, and Dr. Xiuqi Xi for his helpful recommendations. The computational fire modelling with FDS in this MPQ was performed using computational resources supported by the Academic & Research Computing group at Worcester Polytechnic Institute (WPI). Lastly, thanks to the Chemical Engineering and Fire Protection Engineering departments at WPI, by which this project was funded.

Abstract

Fire plumes are a very important area of study for many applications, including fire detection, wildfire models, and toxicant dispersal. By understanding the movement of smoke, thermal radiation and temperature gradients through plume studies, fire behavior can be better predicted, prevented, and controlled for the purposes of life safety. In this report, plume theory will be summarized to serve as the basis for a fire dynamics class module, and an assignment prompt is developed for the module. It will use experimental data and a computational model simulation, both of which were performed in this study. The experimental data consists of two gasoline pool fires, 0.25 and 1.0 meters in diameter. The objectives of the class module that are reached with the assignment prompt, are listed below:

1. Students will implement plume theory to calculate fire characteristics, including flame height, centerline temperature, centerline velocity and plume width.
2. Students will validate the theoretical plume correlations using data from computational models and experiments.
3. Students will visualize the plume characteristics to better their understanding.

Table of Contents

List of Figures

List of Tables

1. Motivation: New Fire Dynamics Course Module

FP 521 Fire Dynamics is a core class required for all Fire Protection Engineering Masters students at Worcester Polytechnic Institute (WPI). One fundamental module of the course is on fire plumes. This module involves defining the structure of a fire (flaming, intermediate and plume region), as well as calculating the flame height. While defining each region, students study the trends and relationships of the plume characteristics, including centerline temperatures and velocities, and plume width. These concepts are important baselines when moving further into the course and studying topics like zone modeling for compartment fires and understanding smoke levels in a compartment.

At the time of this project, the class module does not involve the use of lab experiments or computational models to demonstrate the characteristics of a fire plume. The goal of this project is to modernize the module by connecting theoretical curves with experiments and models. This project achieves this goal by involving the use of experiments performed in WPI's UL Fire Protection Engineering Performance Lab and a computational model performed in Fire Dynamics Simulator (FDS), as well as organizing and improving the module contents using new educational tools and a new assignment prompt.

2. Background

2.1 Plume Theory

A fire plume is the result of buoyancy due to temperature differences in the air; the hot gases and smoke are much less dense than the ambient air, causing the gases to rise rapidly. The gases rise most often in a turbulent flow. Even a small candle that has a smooth flame may initially have a laminar plume, but as the plume rises it becomes turbulent. Although often not visible to the human eye, using Schlieren imaging, Figure 1 below shows the plume flows the turbulence of a candle. These turbulent fires can be distinguished by an unsteady flame tip and the visible oscillations that shed from the plume, called eddies.

Figure 1. *Fire plume of a candle visualized using Schlieren imaging.* [1]

For the purposes of many models and correlations, an open pool fire is used as a standard because it represents a simplified version of many fires. The structure of an open pool fire typically involves a circular pool of fuel, sparked to ignite in an open space. As the fuel burns, the total chemical heat release rate can be calculated using the heat of combustion of the fuel, ΔH_c, and the burning rate, $\dot{m}$, as demonstrated in equation (*1*). In other words, the total heat release rate, $\dot{Q}$, represents the heat released for an ideal and complete combustion. A combustion efficiency factor, X_{eff}, can be used to account for an incomplete combustion process.

$$\dot{Q} = X_{eff}\Delta H_c \dot{m} \tag{1}$$

A percentage of the heat released is emitted in the form of radiation, which is called the radiative fraction, X_r. The remaining heat percentage, or the convective heat fraction, X_c, is used to heat the product gases.

There are fundamentally two main sections of a fire plume, as shown in Figure 2: near-field, or the flame combustion region, and far-field, or the plume. The far-field plume begins at the tip of the flame. Plume characteristics in the two regions, like temperature or flow velocity, follow different trends, so when studying a plume, it is important to know where each region is located. Region separation is defined by the flame height. Because the tip fluctuates, measurements are taken as an average flame height, L_f. The average is found by determining at what height the flame

luminosity intermittency is at 50%. [2] This average tends to be slightly lower that what is perceived by the human eye. [3]

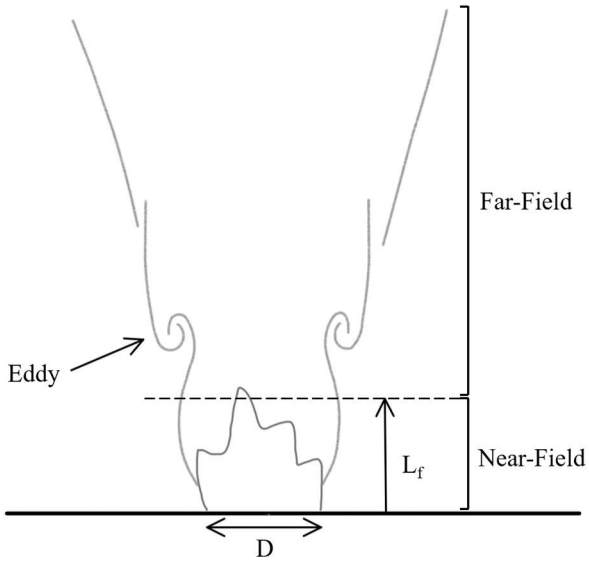

Figure 2. *Basic pool fire structure.*

When using computer modeling systems, like Fire Dynamics Simulator (FDS), the flame height is not defined in this way. Instead, the height is determined by the centerline point at which 97% of the fire's heat has been released. [4]

Multiple experimental correlations for flame height have been formulated, which are often represented using normalized flame characteristics. A well acknowledged correlation created by Heskestad in 1984 is shown below. [5]

$$\frac{L_f}{D} = -1.02 + 15.6N^{1/5} \tag{2}$$

Where L_f is flame height and D is the effective diameter of the fuel source. N is defined below, where ΔH_c is heat of combustion, r is the mass stoichiometric ratio of air to fuel, and $\dot{Q}$ is total heat release rate.

$$N = \left[\frac{c_p T_\infty}{g\rho_\infty^2 (\Delta H_c / r)^3}\right]\frac{\dot{Q}^2}{D^5} \tag{3}$$

Another similar form of this equation is presented below, using a variable A.

$$L_f = -1.02D + A\dot{Q}^{2/5} \tag{4}$$

$$A = 15.6\left[\frac{c_p T_\infty}{g\rho_\infty^2(\Delta H_c/r)^3}\right]^{1/5} \tag{5}$$

$\Delta H_c/r$ is the heat released per unit mass of air entering the combustion reaction. For most gas and liquid hydrocarbon fuels, $\Delta H_c/r$ remains within 2900 – 3200 kJ/kg. [6] This means under normal atmospheric conditions, A falls within a range of 0.226 – 0.240 ($mkW^{-2/5}$). Therefore, to simplify the equation, a commonly used value of A is 0.235.

$$L_f = -1.02D + 0.235\dot{Q}^{2/5} \tag{6}$$

A similar, nondimensionalized equation using $\dot{Q}^*$, a normalized heat release rate derived by Zukoski in 1975, shown below. [6]

$$\frac{L_f}{D} = 3.7\dot{Q}^{*2/5} - 1.02 \tag{7}$$

$$\dot{Q}^* = \frac{\dot{Q}}{\rho_\infty c_p T_\infty \sqrt{g} D^{3/2}} \tag{8}$$

Equation (7), developed by McCaffery, is proved to be adequate for flames with $\dot{Q}^* > 0.2$, however as demonstrated in Figure 3,the correlation breaks down for small $\dot{Q}^*$ values. [7]

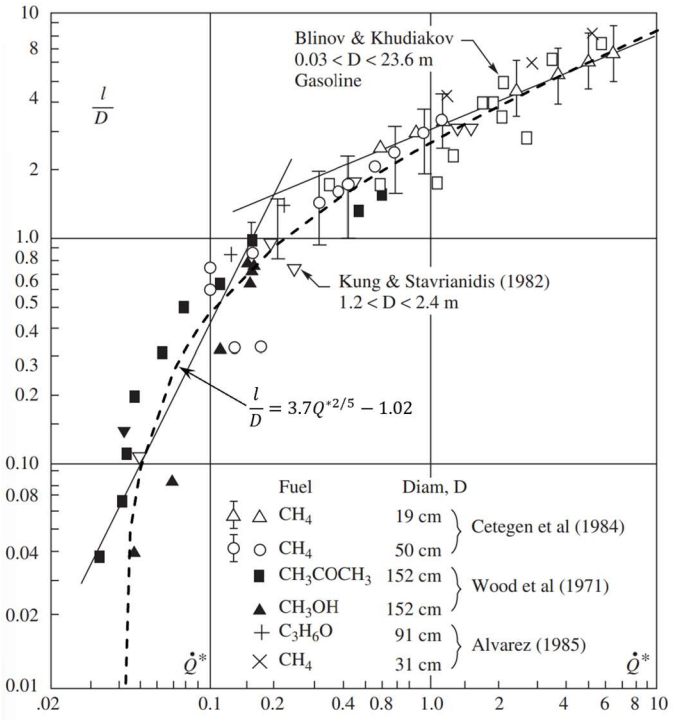

Figure 3. *Flame height trends, taken from Drysdale.* [7]

It is important to note that there are some inconsistencies found in literature. For example, Drysdale presents equations (6)(7) and (8) in terms of the convective heat release rate, Q_c, rather than the total heat release rate, $\dot{Q}$. [7] Many more flame height correlations exist by different fire researchers, including the following equation for flame height in air from Quintiere in 1998. [3]

$$\dot{Q}^* = 0.0059\left(\frac{\psi^{3/2}}{1-X_r}\right)\left(\frac{L_f}{D}\right)^{1/2}\left[1+0.357\left(\frac{L_f}{D}\right)\right]^2 \tag{9}$$

$$\psi = \frac{(1-X_r)\Delta H_c}{c_p T_\infty r} \tag{10}$$

Below, Figure 4 demonstrates the differences in trends for these correlations, as well as experimental data recorded at atmospheric conditions.

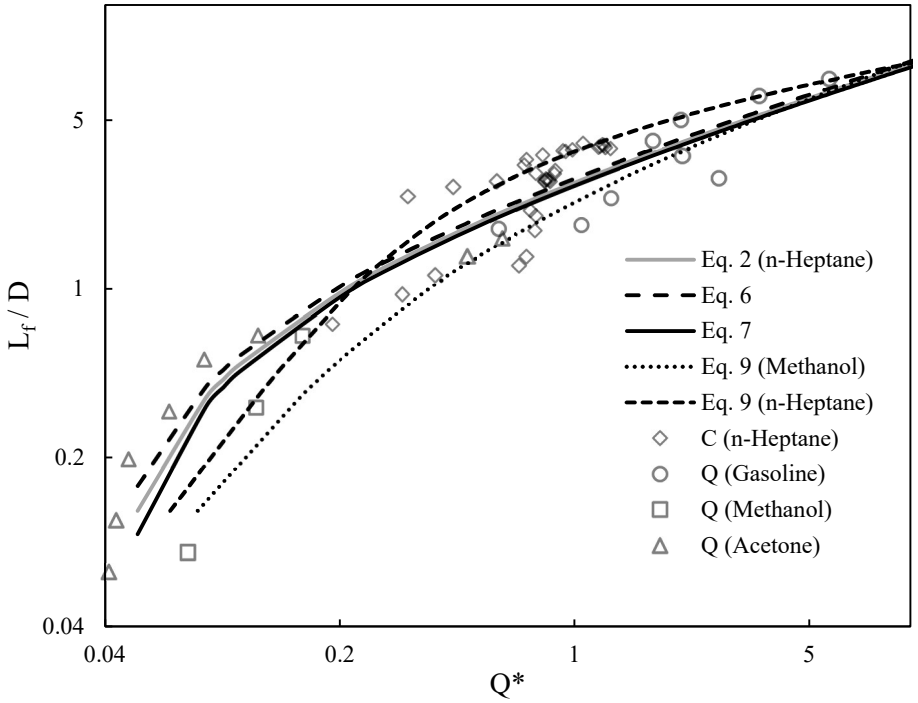

Figure 4. *Flame height correlations and experimental data from Quintiere (Q) and Chen (C).* [3], [8]

Because of the turbulent nature of the flames, these correlations will often not find the exact height, as shown by comparing the experimental data in Figure 4. However, the experimental points follow and surround the trendlines, which validate that the relationships are adequate for fire calculations, but also have limits in their accuracy. While equations (6) and (7) are appropriate correlations for typical fires at atmospheric conditions, Heskestad's original correlation (2) has

proved to better account for fires at a large range of ambient temperatures, and therefore N is considered a more accurate scaling parameter. [6]

Other characteristics that are important for modeling a plume include temperature, T, velocity, u, and plume width, b as a function of z. As demonstrated in Figure 5, temperature and velocity horizontal profiles often follow a Gaussian trend, and at the plume centerline is the peak value. Centerline plume values are denoted by a "0" subscript.

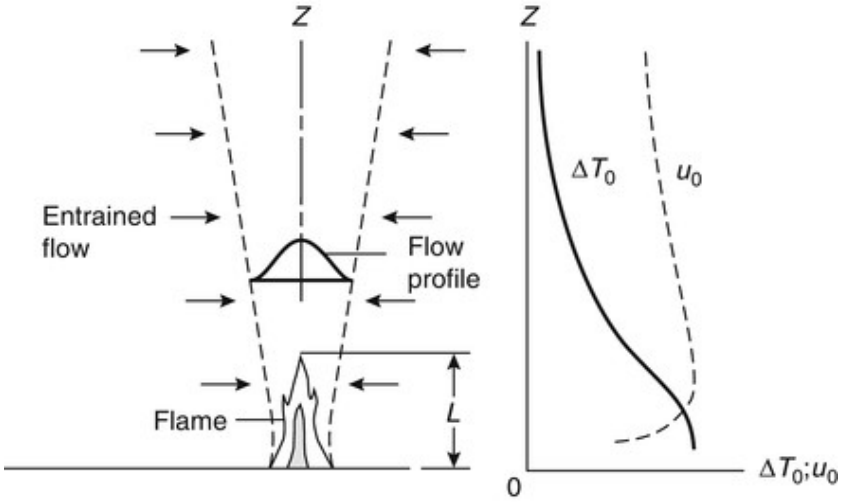

Figure 5. *Axial temperature and velocity profiles of a turbulent fire plume. Taken from Heskestad.* [6]

Centerline temperatures and velocities of a fire behave differently in near-field compared to far-field. The following equations have been developed by Heskestad [5] for far-field plumes 1984.

$$b_{\Delta T} = 0.12\left(\frac{T_0}{T_\infty}\right)^{1/2}(z - z_0) \tag{11}$$

$$\Delta T_0 = 9.1\left(\frac{T_\infty}{g c_p^2 \rho_\infty^2}\right)^{1/3} \dot{Q}_c^{2/3}(z - z_0)^{-5/3} \tag{12}$$

$$u_0 = 3.4\left(\frac{g}{c_p \rho_\infty T_\infty}\right)^{1/3} \dot{Q}_c^{1/3}(z - z_0)^{-1/3} \tag{13}$$

The plume radius, $b_{\Delta T}$, is defined at the point the temperature rise has declined to $0.5\Delta T_0$. $\dot{Q}_c$ is the convective heat release rate and z_0 is the virtual origin of the fire, or the theoretical point source height, often below the fire source. In these equations, the height above the fuel is replaced by $(z - z_0)$, which represents distance from the virtual origin. A negative origin represents a point below the fuel, like shown in Figure 6.

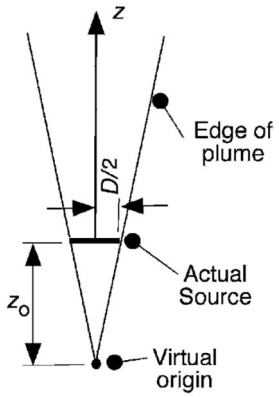

Figure 6. *Virtual origin, taken from Quintiere.* [3]

The virtual origin can be calculated using one of the equations below. [3], [6] However, similar to equations (6) and (8) previously mentioned, Drysdale uses the convective heat release rate, Q_c, rather than the total heat release rate, $\dot{Q}$, when calculating the virtual origin. [7]

$$z_0 = -1.02D + 0.083\dot{Q}^{2/5} \tag{14}$$

$$z_0 = -1.02D + (1.38D)Q^{*2/5} \tag{15}$$

An alternative method for calculating plume characteristics was presented by Quintiere in 1998 [9], in which relationships were developed for both near and far-field, as well as between axisymmetric and infinite line plumes. An axisymmetric flow model is one where the flow variables, like temperature and velocity, do not change with the angular coordinate, θ. The infinite line source model presents radial heat transfer from a centerline (z-axis), as if there is a cylindrical tube of infinitely small radius that acts as a heat source.[10] These relationships use a series of nondimensionalized terms as listed below.

$$\Phi = \frac{T_0 - T_\infty}{T_\infty} \tag{16}$$

$$\mathrm{W} = \frac{u_0}{\sqrt{g z_c}} \tag{17}$$

$$\mathrm{B} = \frac{b}{z_c} \tag{18}$$

$$\zeta = \frac{z}{z_c} \tag{19}$$

$$z_c = \left(\frac{\dot{Q}}{\rho_\infty c_p T_\infty \sqrt{g}}\right)^{2/5} \tag{20}$$

Where z_c is the characteristic length scale for a plume. Quintiere used a series of data from available literature to develop the numerical coefficients and correlations shown in Table 1 and Table 2. A radiative fraction is listed as a representation of the recorded fires used to formulate the equations.

Table 1. *Near-field plume correlations developed by Quintiere* [9]

Dimensionless Variable	Axisymmetric ($X_r = 0.20$)	Infinite Line ($X_r = 0.30$)
Φ	0.347ψ or 2.73	0.450ψ or 3.1
W	$0.720(\psi\zeta)^{\frac{1}{2}}$ or $2.02\left(\zeta^{\frac{1}{2}}\right)$	$0.877(\psi\zeta)^{1/2}$ or $2.3\left(\zeta^{\frac{1}{2}}\right)$
B	0.179ζ	0.444ζ
$\frac{W^2}{\Phi\zeta}$	1.50	1.41

Table 2. *Far-field plume correlations developed by Quintiere* [9]

Dimensionless Variable	Axisymmetric ($X_r = 0.20$)	Infinite Line ($X_r = 0.30$)
Φ	$10.58(1 - X_r)^{\frac{2}{3}}\left(\zeta^{-\frac{5}{3}}\right)$	$3.30(1 - X_r)^{\frac{2}{3}}(\zeta^{-1})$
W	$4.17(1 - X_r)^{\frac{1}{3}}\left(\zeta^{-\frac{1}{3}}\right)$	$2.25(1 - X_r)^{\frac{1}{3}}$
B	0.118ζ	0.103ζ
$\frac{W^2}{\Phi\zeta}$	1.64	1.54

An example of these correlations can be found below in Figure 7, using an example pool fire of gasoline in a 0.5 meter diameter pool. There are two trends, near and far field, for all three characteristics (centerline temperature, centerline velocity and plume width).

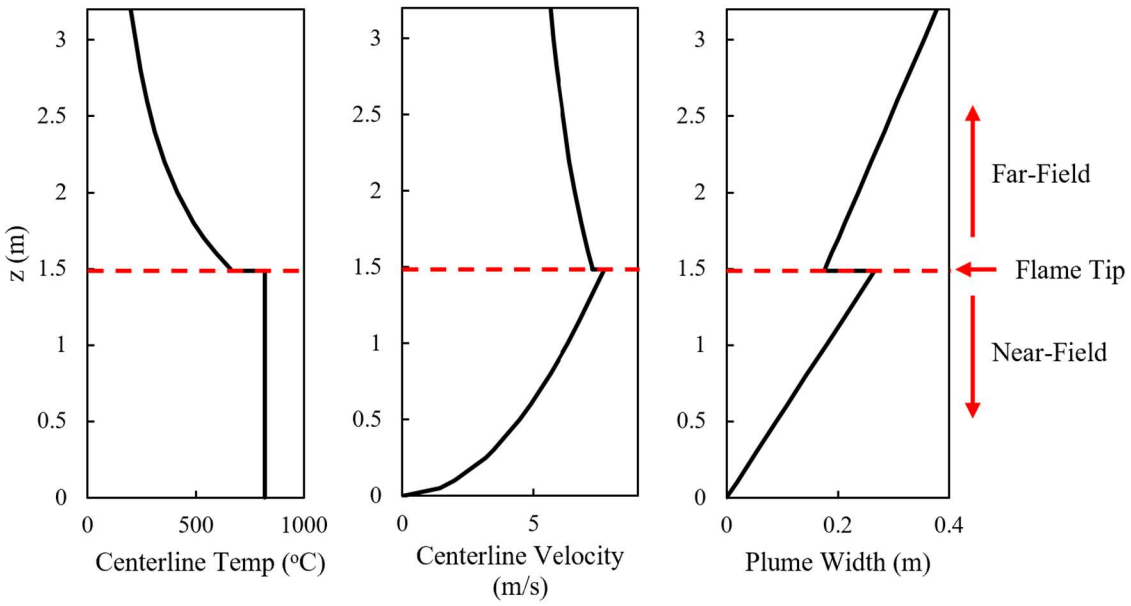

Figure 7. *Quintiere axisymmetric plume correlations for a 0.5 m diameter gasoline pool fire.*

2.2 Computational Modeling of Fire Plumes

Studying fire plumes is important for computational modeling efforts because fire plumes are present in many fire scenarios, and they can be used as a standard reference fire to validate fire models. These computational fire modelling methods use computational fluid dynamics (CFD) as a basis to model the buoyant, turbulent flames and smoke movement. Early fire models used Reynolds Averaged Navier–Stokes (RANS), however these models generally predict jet flames with a higher accuracy than buoyant flames and did not well predict the effects of puffing (eddy shedding). [11][12] The two main numerical turbulence models used today are DNS (direct numerical simulation) and LES (large eddy simulation). These models have many useful applications, like research and design. DNS is often used for research purposes to analyze small scale precise flows that are difficult to measure in a lab. LES has capabilities to analyze large scale fires for buoyancy driven turbulent flows in reasonable timeframes.

DNS requires numerically solving the three-dimensional and time dependent fluid flows directly from the Navier-Stokes equations. This provides a thorough calculation and accurate predictions; however, it requires an immense amount of computational power for many practical problems. According to Doran, “at relatively low Reynolds numbers, typical DNS calculations involve resolution of between 5 million and 20 million nodes in the flow field and require 250 to

400 hours of expensive supercomputer time." [13] As the Reynolds number increases, so does the computational power necessary. Therefore, DNS is logistically limited to low Reynolds numbers, and is ultimately impractical for most applications until computational power available increases. [6]

Fire Dynamics Simulator (FDS) is a fire CFD modelling software developed by the National Institute of Standards and Technology (NIST), which uses LES as the principal technique (with optional DNS mode). This method accounts for eddy shedding, unlike RANS, and requires much less computing power than DNS. The main assumption used in LES is that eddies account for almost all the mixing, and the small-scale eddy motion is considered negligible. [14] LES uses the same base equations as DNS, but by neglecting small-scale turbulence it is a much more cost/time effective method, and for this reason is most common in current models.

2.3 Grid Resolution

For all types of computational modeling, it is important to consider the effects of grid resolution on calculation accuracy and computational time. If the grid resolution is too low, results may be incorrect; if the grid is too high, computation time can be far too long than would be reasonable. But there is no one resolution that will work for every model. In addition to time and accuracy, the size of a fire is a key factor for determining resolution. As the intensity of a fire grows, velocities increase causing more turbulent mixing. This requires a finer resolution to obtain an accurate result. The FDS Validation Guide provides recommended length scale resolutions using a characteristic fire diameter, described below. [15]

$$D^* = \left(\frac{\dot{Q}}{c_p \rho_\infty T_\infty \sqrt{g}}\right)^{2/5} \tag{21}$$

Buoyant pool fire models using LES are recommended to keep $D^*/\delta x$ within a range of 5 to 20, where δx is grid cell length. [16] This range has been determined using a series of previous tests where the FDS model was validated. In other words, a user quantified the model uncertainty and decided the model was appropriate. During this study, a grid sensitivity analysis was performed with the goal to determine a grid resolution for an FDS test in which accurate fire plume data can be extracted for an open pool fire in a practical amount of time for a college class project.

3. Literature Review

3.1 Fire Plumes in Structure Fires

Studying the plume structure of an open pool fire is an important tool for understanding more common and complex applications. For example, when dealing with structure fires, the plume properties affect the compartment smoke levels, detection speed, and the heating of structural materials. A burning fire in a structure is also affected by the constraints of the compartment and behaves differently than an open pool fire. A significant difference between an open fire and a compartment fire is the impact on air entrainment.

Zone models can be used to study airflows in compartment fires. For example, a two zone model of a compartment fire consists of the flame, plume, and smoke buildup at the ceiling in one zone, and the surrounding cool air is the second zone. [3] Within the smoke zone, as the plume comes in contact with the ceiling it creates a ceiling jet (deflected horizontal flows of combustion products). [7] Ceiling jets are important to understand because they spread heat and smoke toward detection devices and initiate the activation of suppression devices. Other important air flows that affect the plume are shown in Figure 8. The hot combustion products rising in the buoyant plume, $\dot{m}_f$, causes the entrainment of cool air toward the flame, $\dot{m}_e$. In addition, other mixing processes occur in the room where the smoke from the plume rapidly enters the ceiling layer, $\dot{m}_1$, and at the air to smoke interface, $\dot{m}_2$. Although, $\dot{m}_2$ is often considered negligible. [17]

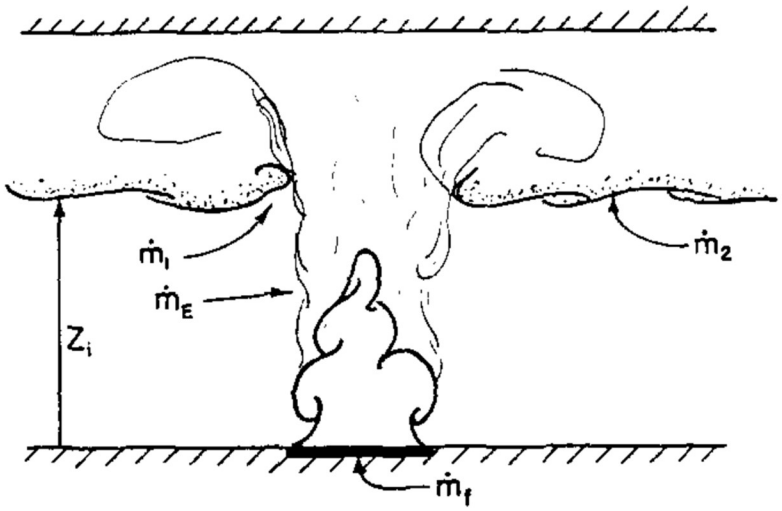

Figure 8. *Air flows in a compartment fire, taken from Zukoski.* [17]

Compartments often affect fire plumes by limiting the air flows. An under-ventilated compartment occurs when there is not enough oxygen present to meet the stoichiometric demand of combustion. [18] The equivalence ratio (Φ) of a fire, defined in equation (*22*), characterizes the available oxygen for a fire.

$$\Phi = \frac{actual\ fuel\ to\ air\ ratio}{stoichiometric\ fuel\ to\ air\ ratio} \tag{22}$$

When Φ<1 the compartment is well ventilated and when Φ>1 the compartment is under-ventilated. One result of a low ventilated fire is an increase in toxic products, like carbon monoxide (CO) and hydrogen cyanide (HCN). Figure 9 below is from a study performed by Purser that shows this relationship, showing the CO mass fraction with change in the equivalence ratio. [19]

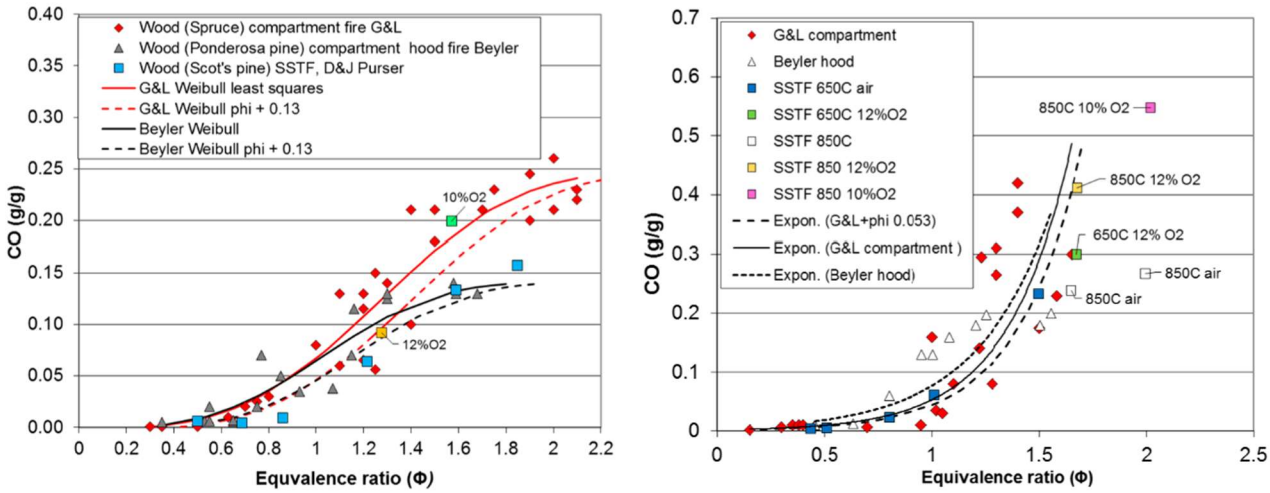

Figure 9. *Mass fraction of CO produced with changes in equivalence ratio, including results from wood and PMMA respectively. Taken from Purser.* [19]

The location of a fire in a compartment also affects the plume. When a fire is located adjacent to a wall or a corner, the air entrainment is more limited than in the center of a room. Figure 10 below is from a study performed by Wang, in which a square propane burner was placed in varying locations of a compartment with a single vent. [18] This study shows that, just as discussed with an under ventilated compartment, when a fire is restricted by a wall or corner, a greater concentration of CO is produced, and less oxygen can be entrained and consumed by the fuel.

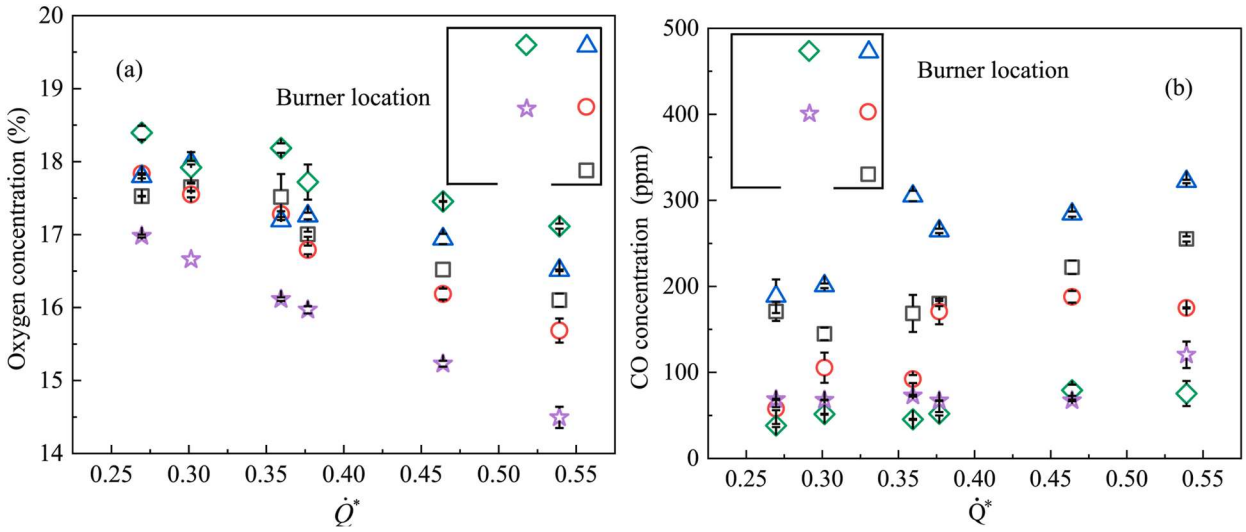

Figure 10. *Effects of fire location in a compartment on oxygen and CO concentration. Taken from Wang.* [18]

3.2 Fire Plumes in Wildfires

Fire plume studies serve as a basis for understanding the movement of smoke, and another very important application for smoke movement is wildfires. The smoke movement influences the spread of wildfire, as well as the spread of toxicants. Data from 1997 through 2006 shows that an estimated 340,000 annual deaths globally are attributable to smoke from landscape fires, and climate changes are likely to cause this number to increase as years go on. [20] There are four factors that allow for a wildfire to start: ignitions, continuous fuels, droughts, and weather conditions (such as high temperatures, low humidity, and wind). [21] As the climate changes, prolonged periods of hot days increase drought periods and cause a higher flammability of landscapes. [22]

While climate change can affect the severity of wildfires, large wildfires can also negatively impact the atmosphere. Small smoke aerosols emitted from a fire can rise into the atmosphere and stay there for weeks to months. [23] For example, the significant fires in western North America have similar effect to a moderate volcanic eruption. [23] Some toxicants that can spread to the atmosphere include carbon dioxide and nitrogen oxides for dry fuels, but partial oxidization and less complete combustion results in products such as carbon monoxide, hydrogen cyanide and ammonia. [23] During the 2020 wildfires in California, there was intense pollution that spread throughout western United States. AirNow is a website run by the US Environmental Protection

Agency (EPA) that records air quality in the United States, including particle pollution. Figure 11 below is the air quality recorded in September of 2020, largely measuring PM, or particulate matter; PM10 is a measure of particles with a diameter of 10μm or less, and PM2.5 is a measure of particles with a diameter of 2.5μm or less. The resulting Air Quality Index (AQI) is a measure of air safety on a scale of 0 to 500.

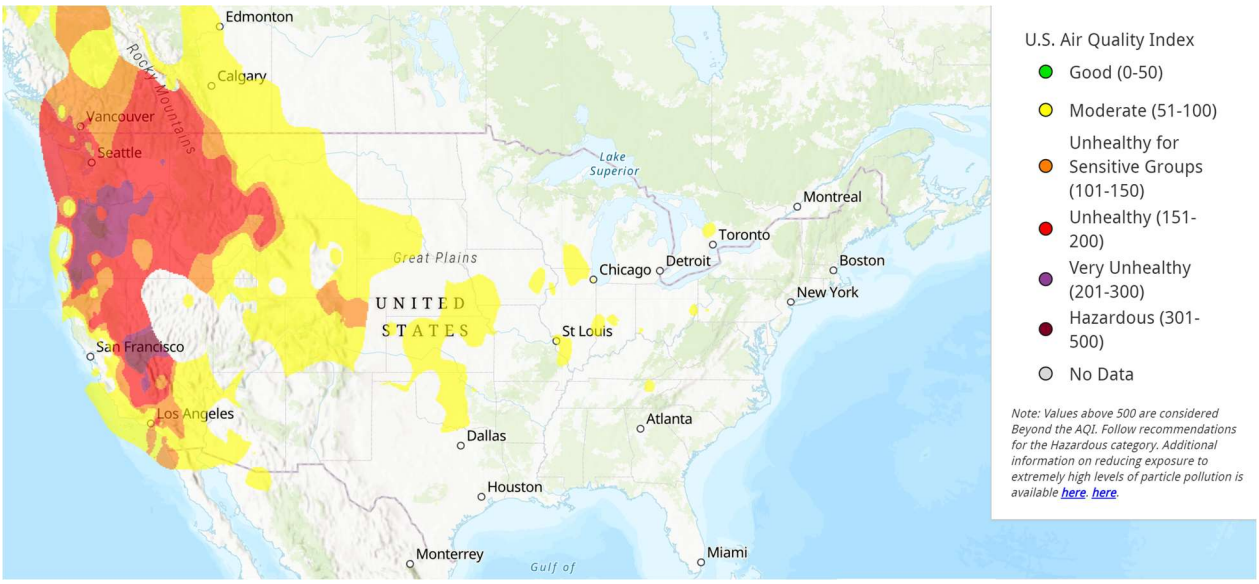

Figure 11. *Air quality (measured by PM2.5 and PM10) recorded by AirNow on September 16, 2020.* [24]

Smoke transport, like that seen in California, can be attributed to multiple factors including fire intensity (heat release rate) and injection height, or the height at which the smoke plume begins to spread horizontally. [25] Just as demonstrated with a pool fire, fires with greater heat release rates cause higher temperature gradients and drives the buoyant plume to a higher velocity, resulting in larger injection heights. This is demonstrated in Figure 12. In addition to fire intensity, the stability of atmospheric conditions influences smoke distribution, also demonstrated in Figure 12. A stable atmosphere is one where temperatures gradually decrease with height, and an unstable atmosphere is one where temperatures rapidly decrease with height.

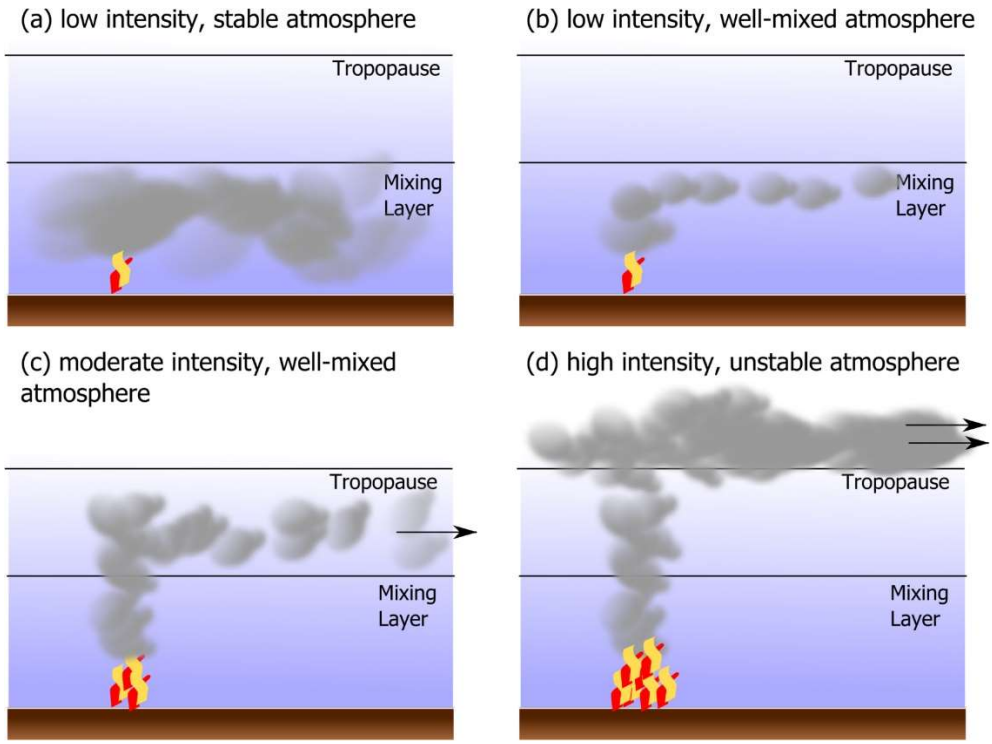

***Figure 12**. Examples of smoke dispersion, taken from Williamson.* [25]

Fire plumes are not only studied for the spread of smoke and toxins, but also for the spread of flame. The plume of a wildfire can carry and transport firebrands, or embers, which can land on an ignitable surface to cause a spotfire, which is a significant mechanism for fire spread. [22] During the Witch and Guejito California wildfires of 2007, firebrand attacks are responsible for 2/3 of the destroyed homes. [26] Firebrand propagation can be separated into three different factors: generation, transport, and ignition of exposed fuel. [27] Transport is largely affected by two main factors: wind and the convective plume. Wind is responsible for most short range transport, which requires little to no lofting. When the convective plume lofts firebrands slightly before it is carried away by wind, it can be described as medium range transport. Lastly, long range transport occurs when a firebrand is lofted throughout the fully developed plume before getting carried away by wind. [22] Figure 13 demonstrates the effects of the wind and plume forces on the trajectory of a fire brand.

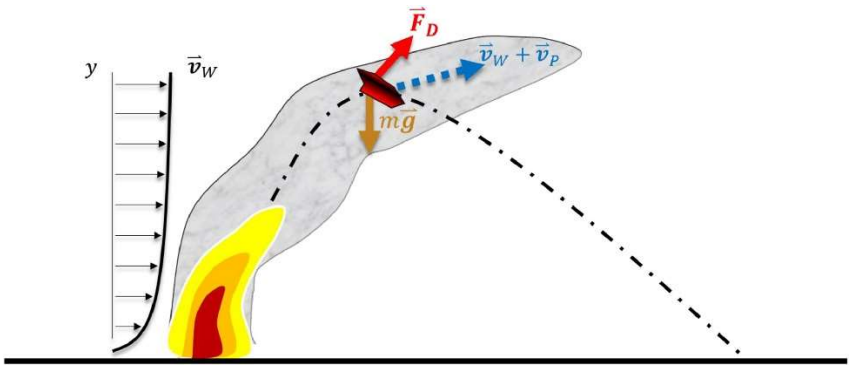

Figure 13. *Schematic of a firebrand trajectory, taken from Manzello.* [28]

Wind is a very important factor of fire weather, or the weather conditions directly affecting fire behavior. As discussed, it affects the spread of smoke and fire brands. However, it also increases combustion efficiency by feeding oxygen into the fire, and increases evaporation rates, which causes the landscape to dry and increase flammability of fuels. [21] When a fire is so intense that it creates its own winds due to the air entrainment process, it is described as a firestorm. Another phenomenon that can occur due to wind and plume air entrainment is a fire whirl, depicted in Figure 14.

Figure 14*. Fire whirl image captured by fire fighter Charles Bolt.* [29]

As air is entrained into the buoyant fire plume, it may intensify due to tangential velocity around the fire. This can generate the swirling flames of a fire whirl due to high angular velocities,

which results in unusually high flame heights and vertical velocities. [30] This is a very dangerous wildfire action because it increases the effect of firebrand transport and can cause a faster spread of fire.

4. Gasoline Pool Fire Experiment Setup

For this study, two gasoline open pool fires with differing pool sizes were burned and analyzed. The small-scale pool fire has a 25 cm diameter pool and a thermocouple tree to measure the centerline temperature of the fire plume. The large-scale pool fire has a 1 meter diameter pool and will not have a thermocouple tree because the plume is too large for a reasonable thermocouple tree to be used.

4.1 Small-Scale Pool Fire Setup

For the small-scale fire, a 25 cm carbon steel tray was placed on an insulated load cell. A load cell, with a resolution of 1 g and about 0.1 seconds was used to measure the mass loss rate (MLR) of fuel throughout the burn. A thermocouple tree made of 80/20 aluminum material had eleven 3-ft long threaded rods reaching to the plume centerline, each holding a K-type 24-guage (0.54 mm diameter) thermocouple. Using equation (7) and a MLR of 0.055 kg/m^{2}s[7], the estimated steady state flame height is 0.614 m. To find the centerline temperature at and above the flame height, the thermocouple rods will be spaced evenly between 0.6 and 1.6 meters above the base of the fuel tray (10 cm apart). More detailed images for thermocouple tree assembly can be found in Appendix A.

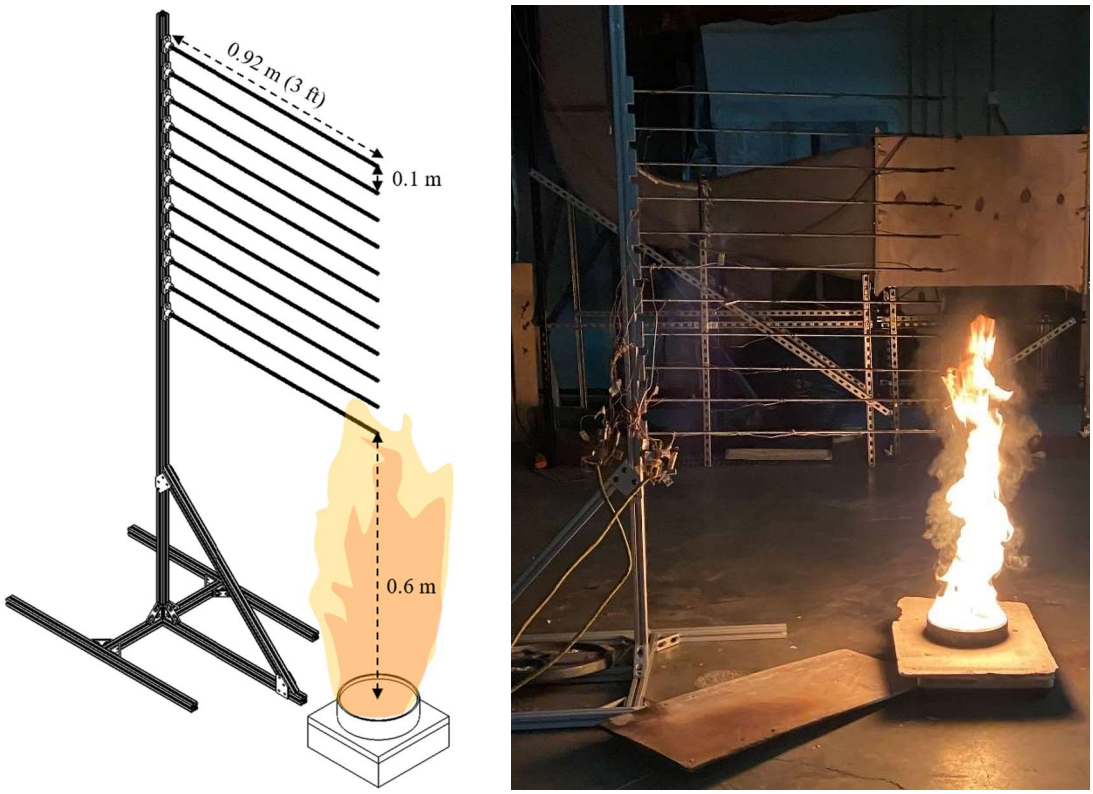

Figure 15. *Small-scale pool experimental setup.*

In addition to what is shown in Figure 15, a camera recorded the burn to determine flame height measurements and to be used as a visual for the class module. To measure flame height, the threaded rods were used as a length scale in the same plane as the fire, based on their known spacing. Using thermocouples, a load cell, and a camera, the following values were collected or calculated to represent a time averaged steady state fire: heat release rate, MLR, flame height, and centerline temperature.

4.2 Large-Scale Pool Fire Setup

The large-scale fire has the same setup as the small-scale, however it does not have a thermocouple tree. The flame height is estimated to be 3.57 m. For the purposes of this experiment, the thermocouple tree is omitted because the required size would be unreasonable to build and operate successfully and safely. A 1 meter tray sat on insulation, a plywood board, and the same load cell used for the previous experiment. In addition, a camera was used to measure flame height, using a wood board with marked measurements as a reference length. Using the load cell and

camera, the following values were calculated to represent a time averaged steady state fire: heat release rate, MLR, and flame height. An image of the setup is shown in Figure 16 below.

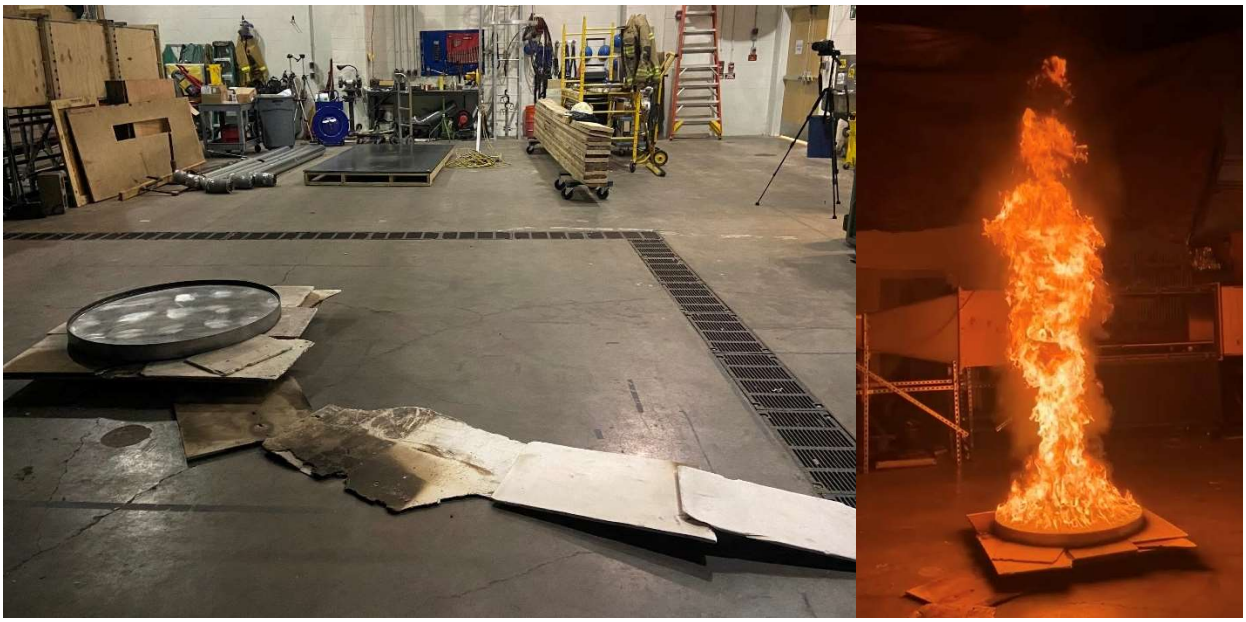

Figure 16. *Large-scale pool experimental setup.*

When fuel trays are used for burning experiments, warping of the metal may cause an uneven surface for the pool. Previous use of the available 25 cm tray did not cause enough warping to warrant purchasing a new tray. However, the available 1 meter tray was too warped to allow for consistent burning as intended. For this reason, a new carbon steel tray was ordered with a new support design to perform this experiment, and is to remain as a resource to the WPI's UL Fire Protection Engineering Performance Lab. It uses 1/8" sheet metal, with a total height of 8 cm and depth of 2.5 cm. An image of this tray is shown in Figure 17 below.

Figure 17. *New carbon-steel, 1 meter fuel tray. Shown are the front and back sides of the tray respectively.*

During the experiments, some warping was observed in the new tray, however it was not enough to affect the burn results. About 2 to 3 minutes of a steady state fire was observed, and an uneven surface was observed as the fire extinguished.

5. Experiment Results

For both size gasoline pools, 3 successful tests were conducted. The small-scale tests averaged about 7.5 minutes of burn time using 400 mL of gasoline and the large-scale tests averaged about 4.5 minutes using 5 L. Below is a summary of the mass loss rates (MLR) measured using the load cell for all tests. These were determined by graphing a trendline of the steady state burning period for each test.

Table 3. *Mass loss rates of each experiment.*

Diameter (m)	Test 1 MLR	Test 2 MLR	Test 3 MLR	Average MLR
0.25	0.0007 kg/s	0.0008 kg/s	0.008 kg/s	0.0077 kg/s
1.0	0.0246 kg/s	0.0245 kg/s	0.0260 kg/s	0.0250 kg/s

Each experiment was recorded by camera, and frames from each steady state burn were used to find flame height in MATLAB, using code provided in FP 4000 – Fire Laboratory course

materials. As shown in Figure 18, the average flame height for the small and large scale fires were found to be 0.822 m and 2.106 m respectively.

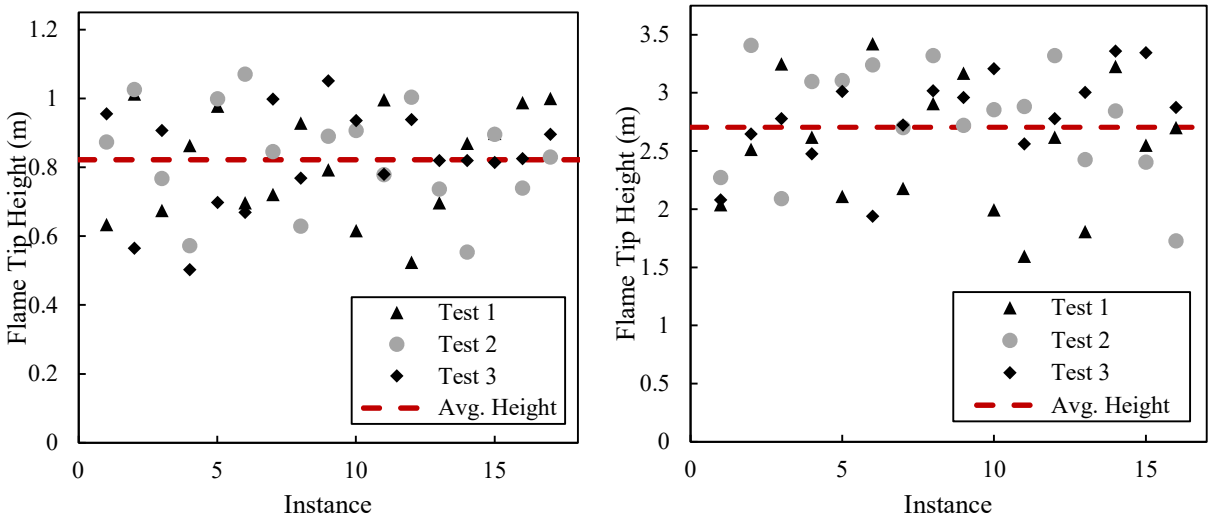

Figure 18. *Flame heights for the small and large scale experiments respectively.*

For the small scale experiments only, centerline temperatures were recorded over time. Figure 19 presents the data recorded during the Test 1 of the burns.

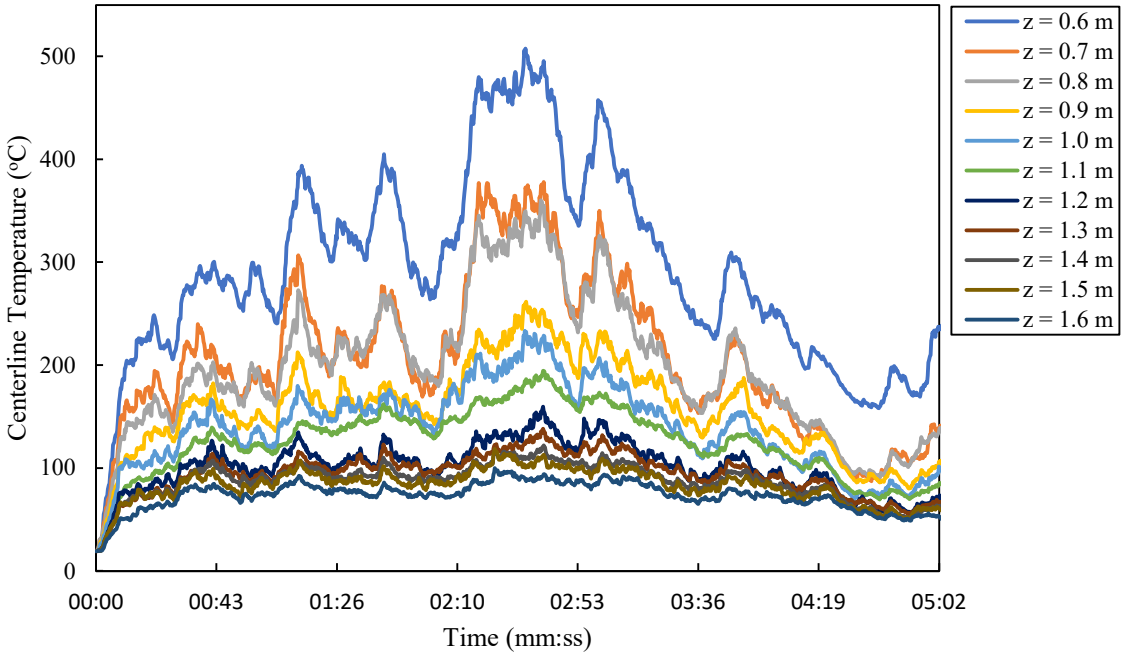

Figure 19. *Centerline temperatures recorded over time for the 25 cm Test 1.*

To better understand the trends of the centerline temperatures, values from each thermocouple was time averaged over a steady state burning period. The results proved to follow the same trend as presented by the far-field axisymmetric plume correlation presented by Quintiere. [9] Thermocouple temperatures were not corrected for radiation losses, which could explain the lower values compared to the Quintiere's correlation. In Figure 20, these results are shown with and without the comparison to Quintiere's correlation.

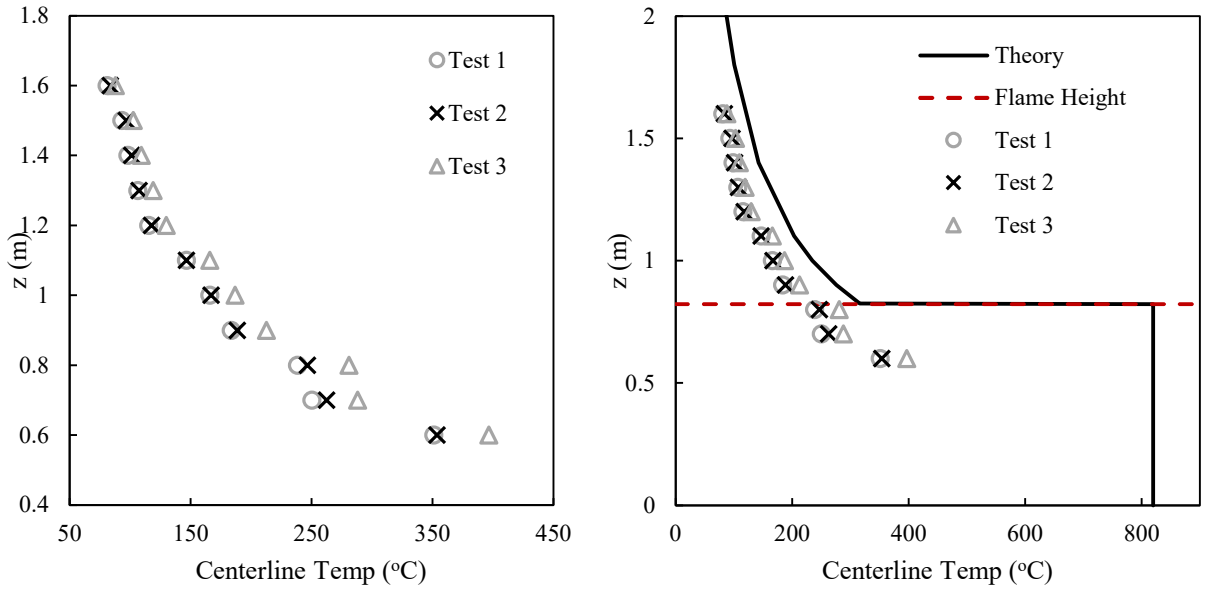

Figure 20. *Steady state centerline temperatures for the small scale fire.*

The tabulated results collected from these experiments will be provided for FP 521 students to use in an assignment prompt provided to them as a part of this project. The data will be used to create similar graphs to those above, to compare Quintiere's correlations, and other results collected in a simulation performed in Fire Dynamics Simulator (FDS).

6. Modeling Fire Plumes with the Fire Dynamics Simulator (FDS)

In addition to a lab experiment, an FDS simulation was run to model fire characteristics that are not easily measured in a lab and to compare to data that was collected in the experiment. This model simulates the same fire as the small-scale gasoline pool experiment.

6.1 Defining the Burner

In the FDS model, the burner is a square rather than a circular pool. Since the shape is different from the lab experiment, there are two potential strategies to define the burner side length while maintaining consistency between the data sets. The area of the square can be maintained between the two shapes; in other words, a square with a 22 cm side length has approximately the same area as a circle with a 25 cm diameter. Or the central profile can be kept consistent by using a square with a 25 cm side length. To determine the ideal side length, both sizes were tested in FDS and compared to Quintiere's centerline temperature and velocity correlations for a 25 cm circular pool. [9] The model uses a radiative fraction of 0.40, as averaged from literature. [31] The results are shown in Figure 21 below.

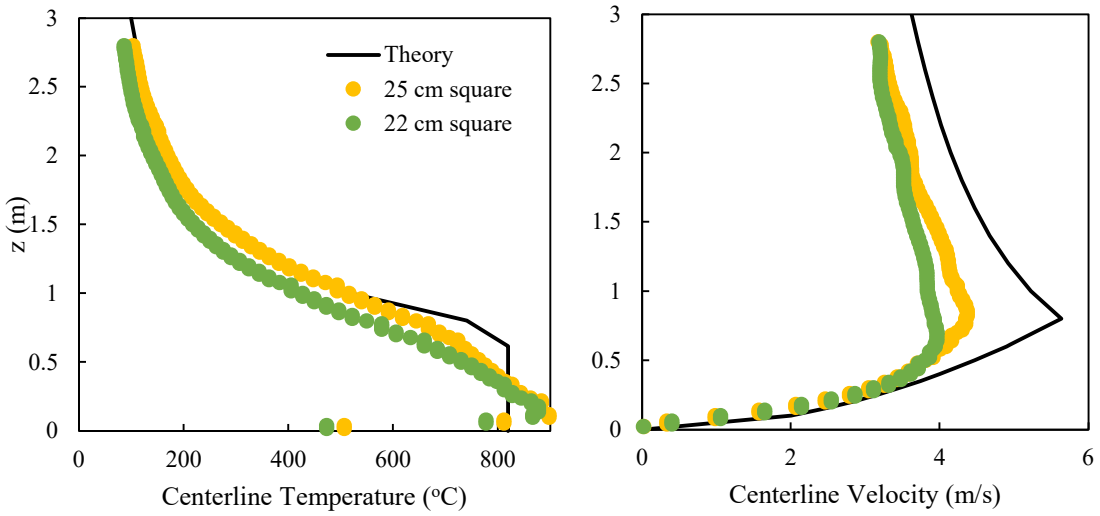

Figure 21. *FDS models using 22 cm sides (maintained area) and 25 cm sides, in comparison to theoretical temperature and velocity correlations using a 0.04 m mesh size.*

Based on these results, the 25 cm side square burner follows both Quintiere's theoretical centerline temperature and velocity trend closer than the 22 cm side. For this reason, a 25 cm square will be used in the FDS model.

6.2 Grid Resolution Test

An important factor to consider for any FDS model is the mesh size, or grid resolution. A mesh size too large may produce inaccurate results, and a mesh size too small may take an unreasonably long time to calculate. As previously mentioned for an open pool fire, $D^*/\delta x$ is recommended to

be within a range of 5 to 20. For this fire, D^* is about 0.409 m. Therefore, the recommended cell length is between the range of 0.020 to 0.082 meters. A grid resolution test was performed to select the ideal mesh size for a model that has a total volume of 1.6 x 1.6 x 3.2 meters. In this test, four models were run using the mesh sizes show in Table 4, as well as the total time the simulation needed to complete the calculations.

Table 4. *Grid resolution test sizes and run times.*

Mesh Size (m)	Mesh Quantity x-axis	Mesh Quantity y-axis	Mesh Quantity z-axis	Elapsed Wall Time
0.02	80	80	160	16.3 hrs
0.04	40	40	80	75 min
0.08	20	20	40	1.9 min
0.16	10	10	20	37 sec

To determine the mesh size that provides the most ideal results, the FDS model centerline temperatures and velocities from the grid resolution study were compared to each other (verification) and were compared to Quintiere's theoretical calculations (validation), in the same manner as the burner size test. Since the correlations represent a steady state fire, the model data was time averaged. To accurately represent a steady state fire, the fire growth stage should be omitted from the data. Figure 22 is a graph of the total heat release rate (HRR) of the fire over time. It is observed that the fire reaches full size after 3 seconds, and therefore the time averaged data will not include the first 3 seconds of the fire model.

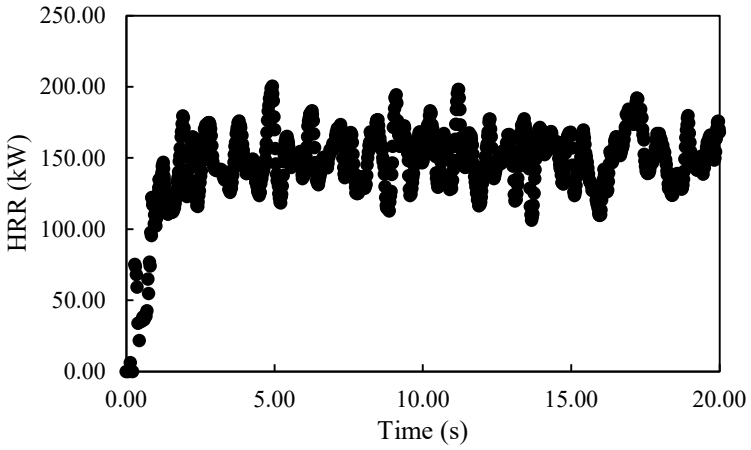

Figure 22. *Total heat release rate over time of a 25 cm gasoline pool FDS model with an 8 mm grid size.*

It is also important to consider the frequency of eddy puffing, to ensure that enough eddies are averaged over time. Pagni developed a relationship between the pool diameter and frequency of eddies, as shown in equation (*23*) below.

$$f = 0.48\sqrt{\frac{g}{D}} \tag{23}$$

Using Pagni's relationship, a 25 cm diameter pool fire will have a frequency of about 3 Hz, or 3 eddies per second. A time range of 3 to 20 seconds was chosen for time averaged data, which will include about 51 eddy occurrences. Taking these factors into account, the grid sensitivity test results are shown in Figure 23 below.

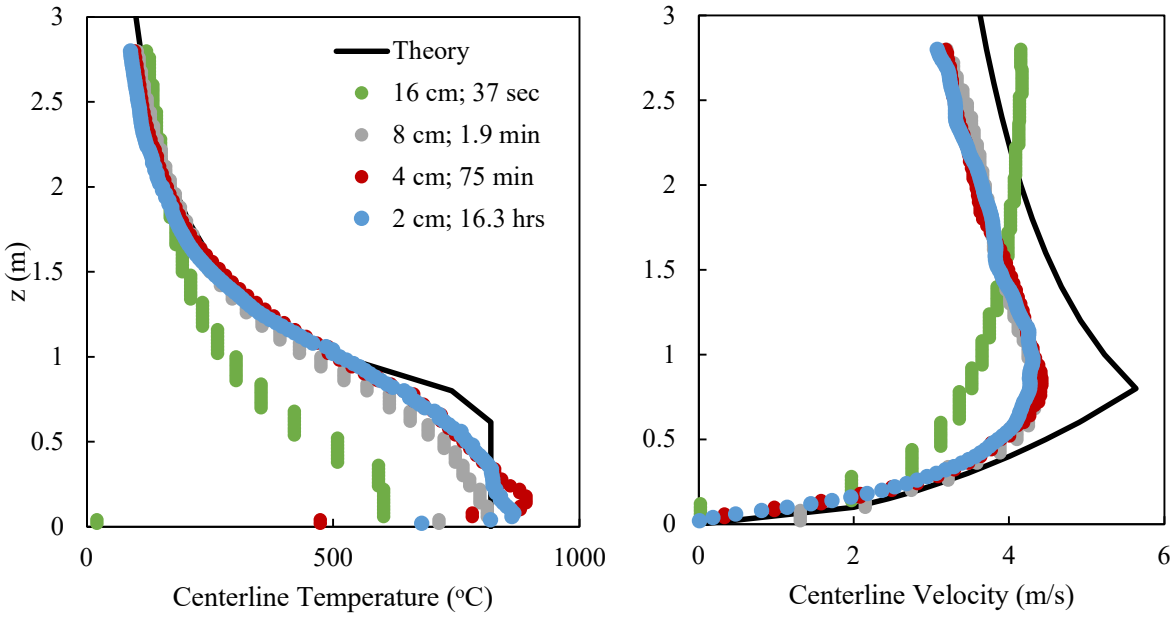

Figure 23. *Grid sensitivity test results.*

All mesh sizes, except for the 16 cm mesh, follow the same trend with minimal variances, and closely align to Quintiere's correlations. Due to the large increase in time scales as the mesh size decreases, the ideal mesh size for the purposes of this project was determined to be 8 cm.

The data collected from the FDS model with an 8 cm mesh will be provided to students in the assignment prompt. The data provided includes HRR and centerline temperature/velocity values for all time steps (up to 20 seconds), at heights from 0.1 m to 3 m with 0.1 m intervals. In addition, the FDS slice file with temperature data at all points in the mesh over all time steps will be given, to determine plume width.

7. Assignment Prompt Development

The purpose of the pool fire experiments, and the computational model is to use the findings for the benefit of WPI's FP521 Fire Dynamics class. Using the experiment and FDS data that is collected, and time averaged, an assignment prompt is put together to achieve the following class objectives.

Objective 1. Students will implement plume theory to calculate fire characteristics, including flame height, centerline temperature, centerline velocity and plume width.

Objective 2. Students will validate the theoretical plume correlations using data from computational models and experiments.

Objective 3. Students will visualize the plume characteristics to better their understanding.

The prompt below will be used in a fire plume class module as a homework assignment to provide practice and aid student understanding by following all objectives.

7.1 Assignment Prompt

The UL Fire Protection Engineering Performance Lab at Gateway Park of WPI houses an open area for the purposes of large fire demonstrations and experiments. The space controls airflow exiting the room through an exhaust hood. This hood is 6 by 6 meters and is located 6 meters above the floor.

Note: Based on safety constraints for the exhaust, the lab space limits fires to have a flame tip below 6 meters and a heat release rate below 3 MW.

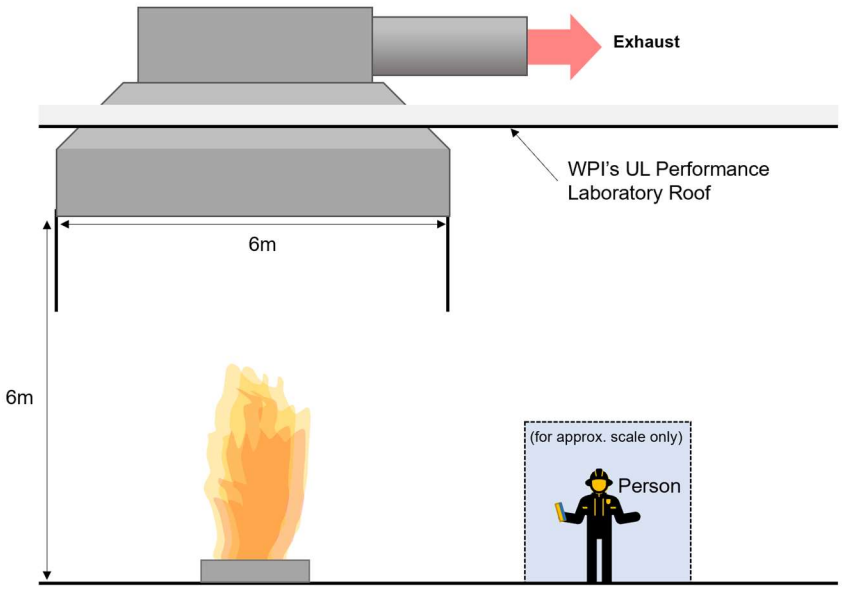

For all flame height calculations, use the following correlation:

$$L_f = -1.02D + 0.235\dot{Q}^{2/5}$$

1. *If you wish to burn an open pool fire in the lab using gasoline, heptane or acetone, estimate the largest diameter pool tray that can be safely burned while staying within the lab constraints for each fuel type. Which safety limit is the constraining factor (flame height or heat release rate)?*

Fuel Type	Heat of Combustion	Mass Loss Rate
Gasoline	44.1 kJ/g	0.055 kg/m^{2}s
Heptane	44.9 kJ/g	0.101 kg/m^{2}s
Acetone	29.1 kJ/g	0.041 kg/m^{2}s

2. *Gasoline is a chemical mixture with varying compositions. This results in uncertainty when defining its chemical properties. Considering a 10% uncertainty of the gasoline heat of combustion listed above, predict a range of total heat release rates and average flame heights for a 1 meter diameter gasoline pool. Find the mass loss rate using data provided in the attached Excel sheet, from a 1 meter gasoline open pool fire experiment.*

a. *In the provided Excel sheet, flame height data collected from open pool fires performed in the WPI fire lab using gasoline. Does the flame height fall within the range of uncertainty? What are some aspects other than chemical composition that can contribute to the uncertainty?*

3. *Now consider a gasoline pool fire with a 25 cm diameter pool, a heat of combustion of 44.1 kJ/g, and a MLR of 0.016 kg/ m^2s.*
    a. *Calculate and graph the centerline temperature, centerline velocity, and plume width of the fire up to 2.5 meters above the fuel using Quintiere's axisymmetric correlations.*

    b. *Provided in an attached Excel sheet is data from a 25 cm gasoline pool fire performed in the WPI fire lab, as well as data from an FDS computational model of the same fire. Graph this data in comparison to the theoretical calculations performed in part a. Because Quintiere's correlations present steady state fires, the data provided is time averaged data during the steady burning period. You should provide 3 resulting graphs:*
        i. *Centerline temperature vs height, including Quintiere's correlations, experimental data, and FDS data.*
        ii. *Centerline velocity (in the z-direction) vs. height, including Quintiere's correlations and FDS data.*
        iii. *Plume width vs. height, including Quintiere's correlations, and FDS data.*

    In all graphs, mark the experimental flame height and the theoretical flame height.

7.2 Reaching Assignment Objectives

All objectives are met with the prompt above. The list below describes how each objective is completed:

Objective 1. This is achieved because each question involves the use of a plume theory equation; all questions involve calculating flame height, and question 3 includes calculating centerline temperature, centerline velocity and plume width.

Objective 2. Reached in both questions 2 and 3. Question 2 involves comparing theory to experimental data and allows for understanding in the uncertainty of many fire calculations. Gasoline is a great example because it is a commonly used, flammable chemical mixture with many variations in composition. Question 3 involves comparing computational model (FDS) data and experimental data to theory. Students will time average raw data provided by the experiment and FDS model to validate the steady state plume correlations. This builds an understanding of how the fire grows over time to reach a quasi-steady state. In addition, it is an example of a sequence of steps that may be taken to process output data received in a model/experiment.

Objective 3. There are multiple ways in which this objective is reached. In the question 1, the use of a lab diagram and using plume characteristics for a practical, on campus application gives an example of the magnitude of fires that can be burned in WPI's UL Fire Protection Engineering Performance Lab, which student have access to use in their education experience at WPI. In addition, question 3 uses a graphical method to visualize the plume characteristics and how they change with height. Finally, a video visual of all experiments will be provided with the module as another visualization method.

8. Conclusion

The goals for this project were to develop educational tools and provide an assignment prompt for the fire plume module of FP 521 Fire Dynamics. This was completed by summarizing important introductory plume theory, collecting experimental data for students to analyze, and modeling a pool fire in FDS for students to analyze.

Two experiments were conducted of varying sizes of gasoline pools, in which centerline temperature, flame height and mass loss rate data were provided as a part of the new assignment prompt. The experiment videos are also available to serve as a visual aid to the learning process in the lecture. In addition, a one meter pool tray and thermocouple tree materials are now provided in the lab for future lab experiments or live demonstrations for FP 521 and other classes. This

project's lab experiments were already incorporated in the FP 3070 class lab demonstration day while this project was being conducted.

An FDS model and its resulting data, including a temperature field, velocity field, and heat release rate over time, is also provided as a part of the new assignment prompt. FDS is a modern tool in active development used at many fire protection engineering companies, and this module now allows for exposure of the program and its comparison to experimental data and theoretical relationships. All files relevant to the assignment prompt were provided as supplemental materials alongside this report to the FP 521 professor, and the advisor of this project, Professor Urban.

9. Nomenclature

b	Plume radius	[m]
B	Dimensionless length parameter	[-]
c_p	Specific heat at constant pressure	[kJ/kg-K]
D	Fuel diameter	[m]
D^*	Characteristic fire diameter	[m]
f	Frequency	[Hz]
g	Gravity	9.81 [m/s^2]
ΔH_c	Heat of combustion	[kJ/kg]
L_f	Flame height	[m]
$\dot{m}$	Mass burning rate	[kg/s]
$\dot{Q}$	Total heat release rate	[kW]
$\dot{Q}^*$	Dimensionless heat release rate	[-]
r	Mass stoichiometric ratio of air to volatiles	[kg/kg]
T	Temperature	[K]
u	Velocity	[m/s]
W	Dimensionless velocity parameter	[-]
X_c	Convective fraction	[-]
X_{eff}	Combustion efficiency	[-]
X_r	Radiative fraction	[-]
z	Vertical coordinate	[m]

Greek Symbols

ρ	Density	[kg/m^3]
Φ	Dimensionless temperature parameter	[-]
ζ	Dimensionless height parameter	[-]
Ψ	Dimensionless combustion parameter	[-]

Subscripts

f	Flame
∞	Ambient conditions
0	Plume centerline
c	Characteristic variable

10. References

[1] M. J. Hargather and G. S. Settles, "Background-oriented schlieren visualization of heating and ventilation flows: HVAC-BOS," *HVAC and R Research*, vol. 17, no. 5, pp. 771–780, 2011, doi: 10.1080/10789669.2011.588985.

[2] B. Karlsson and J. Quintiere, "Enclosure Fire," 1st ed.CRC Press, 1999, pp. 47–80.

[3] J. G. Quintiere, *Fundamentals of fire phenomena*. John Wiley, 2006.

[4] K. McGrattan, S. Hostikka, J. Floyd, R. McDermott, and V. Marcos, "Fire dynamics simulator user's guide," Gaithersburg, MD, 2022. doi: 10.6028/NIST.SP.1019.

[5] G. Heskestad, "Engineering relations for fire plumes," *Fire Saf J*, vol. 7, no. 1, pp. 25–32, Jan. 1984, doi: 10.1016/0379-7112(84)90005-5.

[6] G. Heskestad, "Fire plumes, flame height, and air entrainment," in *SFPE Handbook of Fire Protection Engineering, Fifth Edition*, Springer New York, 2016, pp. 396–428. doi: 10.1007/978-1-4939-2565-0_13.

[7] Dougal. Drysdale, *An introduction to fire dynamics*, Third Edition. Wiley, 2011.

[8] B. Chen, S. Lu, C. Li, Q. Kang, and M. Yuan, "Unsteady burning of thin-layer pool fires," *J Fire Sci*, vol. 30, no. 1, pp. 3–15, Jan. 2012, doi: 10.1177/0734904111415807.

[9] J. G. Quintiere and B. S. Grove, "A unified analysis for fire plumes," *Symposium (International) on Combustion*, vol. 27, no. 2, pp. 2757–2766, Jan. 1998, doi: 10.1016/S0082-0784(98)80132-X.

[10] L. Laloui and A. F. Rotta Loria, "Analytical modelling of transient heat transfer," *Analysis and Design of Energy Geostructures*, pp. 409–456, Jan. 2020, doi: 10.1016/B978-0-12-816223-1.00009-6.

[11] Y. Wang, P. Chatterjee, and J. L. de Ris, "Large eddy simulation of fire plumes," *Proceedings of the Combustion Institute*, vol. 33, no. 2, pp. 2473–2480, Jan. 2011, doi: 10.1016/J.PROCI.2010.07.031.

[12] J. X. Wen, K. Kang, T. Donchev, and J. M. Karwatzki, "Validation of FDS for the prediction of medium-scale pool fires," *Fire Saf J*, vol. 42, no. 2, pp. 127–138, Mar. 2007, doi: 10.1016/J.FIRESAF.2006.08.007.

[13] P. M. Doran, "Fluid Flow," *Bioprocess Engineering Principles*, pp. 201–254, Jan. 2013, doi: 10.1016/B978-0-12-220851-5.00007-1.

[14] K. B. McGrattan, "Fire dynamics simulator technical reference guide volume 1: Mathematical Model," Gaithersburg, MD, 2006. doi: 10.6028/NIST.SP.1018.

[15] K. B. McGrattan, "Fire dynamics simulator technical reference guide volume 3: validation," Gaithersburg, MD, 2006. doi: 10.6028/NIST.SP.1018.

[16] R. J. Mcdermott, "Quality assessment in the fire dynamics simulator: a bridge to reliable simulations," 2011.

[17] E. E. Zukoski, T. Kubota, and B. Cetegen, "Entrainment in fire plumes," *Fire Saf J*, vol. 3, no. 2, pp. 107–121, Jan. 1981, doi: 10.1016/0379-7112(81)90037-0.

[18] D. Wang, X. Ju, and L. Yang, "Experimental studies of the effect of burner location on the development of building fires," *Journal of Building Engineering*, vol. 65, p. 105680, Apr. 2023, doi: 10.1016/J.JOBE.2022.105680.

[19] D. A. Purser, "Toxic combustion product yields as a function of equivalence ratio and flame retardants in under-ventilated fires: Bench-large-scale comparisons," *Polymers (Basel)*, vol. 8, no. 9, Sep. 2016, doi: 10.3390/polym8090330.

[20] F. Johnston *et al.*, "Estimated Global Mortality Attributable to Smoke from Landscape Fires," *Environ Health Perspect*, vol. 120, no. 5, May 2012.

[21] J. G. Pausas and J. E. Keeley, "Wildfires and global change," *Front Ecol Environ*, vol. 19, no. 7, pp. 387–395, 2021, doi: https://doi.org/10.1002/fee.2359.

[22] R. Wadhwani, C. Sullivan, A. Wickramasinghe, M. Kyng, N. Khan, and K. Moinuddin, "A review of firebrand studies on generation and transport," *Fire Saf J*, vol. 134, p. 103674, 2022, doi: https://doi.org/10.1016/j.firesaf.2022.103674.

[23] I. N. Sokolik, A. J. Soja, P. J. DeMott, and D. Winker, "Progress and Challenges in Quantifying Wildfire Smoke Emissions, Their Properties, Transport, and Atmospheric Impacts," *Journal of Geophysical Research: Atmospheres*, vol. 124, no. 23, pp. 13005–13025, Dec. 2019, doi: 10.1029/2018JD029878.

[24] "Interactive Map of Air Quality." AirNow.gov (accessed Apr. 19, 2023).

[25] G. J. Williamson, D. M. J. S. Bowman, O. F. Price, S. B. Henderson, and F. H. Johnston, "A transdisciplinary approach to understanding the health effects of wildfire and prescribed fire smoke regimes," *Environmental Research Letters*, vol. 11, no. 12, Dec. 2016, doi: 10.1088/1748-9326/11/12/125009.

[26] A. Maranghides and W. Mell, "A Case Study of a Community Affected by the Witch and Guejito Wildland Fires," *Fire Technol*, vol. 47, no. 2, pp. 379–420, Apr. 2011, doi: 10.1007/s10694-010-0164-y.

[27] K. Zhou, S. Suzuki, and S. L. Manzello, "Experimental Study of Firebrand Transport," *Fire Technol*, vol. 51, no. 4, pp. 785–799, 2015, doi: 10.1007/s10694-014-0411-8.

[28] S. L. Manzello, S. Suzuki, M. J. Gollner, and A. C. Fernandez-Pello, "Role of firebrand combustion in large outdoor fire spread," *Prog Energy Combust Sci*, vol. 76, p. 100801, 2020, doi: https://doi.org/10.1016/j.pecs.2019.100801.

[29] "Terrifying 'fire whirl' caught on camera by firefighter," *KTVU FOX 2*, Aug. 17, 2016. https://www.ktvu.com/news/terrifying-fire-whirl-caught-on-camera-by-firefighter (accessed Apr. 19, 2023).

[30] K. H. Chuah, K. Kuwana, K. Saito, and F. A. Williams, "Inclined fire whirls," *Proceedings of the Combustion Institute*, vol. 33, no. 2, pp. 2417–2424, 2011, doi: https://doi.org/10.1016/j.proci.2010.05.102.

[31] M. Muñoz, E. Planas, F. Ferrero, and J. Casal, “Predicting the emissive power of hydrocarbon pool fires,” *J Hazard Mater*, vol. 144, no. 3, pp. 725–729, Jun. 2007, doi: 10.1016/J.JHAZMAT.2007.01.121.

11. Appendices

11.1 Appendix A. Thermocouple Tree Assembly

Figure A.1. *Thermocouple tree assembly.*

An image of the full thermocouple (TC) tree is shown above. The center 80/20 aluminum piece was not cut and kept 10 ft tall, for ease of use in future lab construction.

Figure A.2. *Thermocouple tree base.*

Above is a close-up image of the base of the tree. When securing the tree and running experiments, a 45lb weight was placed on the support beneath the 45 degree angled support.

Below is an image of the threaded rods, which are attached to blocks ordered to specifically fit the 3/8” rods. TC wire was attached to the rods using extra scrap TC wire wrapped around the wire and rod. Those TCs, along with extension TC wire, connected to LabVIEW to record the change in temperature over time.

Figure A.3. *TC wire connections.*

Lastly, below is an image of the full setup of the experiment, including the camera and computers.

Figure A.4. *Full setup with TC tree.*

11.2 Appendix B. FDS Input File

```
&HEAD CHID='G08', TITLE='80 mm Grid' /

&MESH IJK=20, 20, 40, XB=-0.8, 0.8, -0.8, 0.8, -0.10, 3.1, / 1.6 x 1.6
x 3.2
&TIME T_END=20. /

&SURF ID='burner', HRRPUA=706, COLOR='RED' / #for gasoline
&OBST XB=-0.125,0.125,-.125,0.125,-.10,0.00,
SURF_IDS='burner','INERT','INERT' / 25cm square
&SPEC ID='LNG', FORMULA='C6.97H14.36'/  #average for Shell A gasoline
is C6.97H14.36O0.15
&REAC FUEL='LNG', RADIATIVE_FRACTION=0.4, HEAT_OF_COMBUSTION=44100. /
#for gasoline

&VENT MB='XMIN', SURF_ID='OPEN' /
&VENT MB='XMAX', SURF_ID='OPEN' /
&VENT MB='YMIN', SURF_ID='OPEN' /
&VENT MB='YMAX', SURF_ID='OPEN' /
&VENT MB='ZMIN', SURF_ID='OPEN' /
&VENT MB='ZMAX', SURF_ID='OPEN' /

&DEVC ID='tmp', XB= 0.00, 0.00,0.00,0.00,0.1,3.0, POINTS=30,
TIME_HISTORY=T, QUANTITY='TEMPERATURE'/
&DEVC ID='vel', XB= 0.00, 0.00,0.00,0.00,0.1,3.0, POINTS=30,
TIME_HISTORY=T, QUANTITY='W-VELOCITY', HIDE_COORDINATES=.TRUE. /
#hide coordinates because both devices use same coordinates
&SLCF PBY=0.0, QUANTITY='TEMPERATURE',VECTOR=.TRUE. /

&TAIL /
```

11.3 Assignment Prompt Deliverable Contents

A folder with all files relevant to the assignment prompt was provided as a supplemental material with the following contents:

- Assignment prompt document.
- Assignment prompt solutions document.
- Assignment prompt excel sheet, with the following tables:
    - MLR Data, 1 meter gasoline pool fire (Question 2)
    - Flame Height Data, 1 meter gasoline pool fire (Question 2)
    - Experimental Temperatures (Question 3)
    - Experimental Flame Height (Question 3)
    - FDS Temperature Data (Question 3)
        - Time averaged points, along x and z axis.
    - FDS Velocity Data (Question 3)
        - Time averaged points, along x and z axis.
- Python file used to extract temperature and velocity data from FDS slice file.

11.4 Appendix D. Budget

Table 5. *Budget.*

Material	Manufacturer	Qty.	Price per Part
45 Degree Flat Plate	80/20	4	$9.42
Corner Bracket	80/20	3	$9.33
Center Tap Base Plate	80/20	11	$16.86
1 Meter Steel Pool Tray	City Welding	1	$523[1]
Total Budget			$300
Total Spent			$251.13
Budget Remaining			$48.87

Note 1: Pool tray was provided by WPI's Fire Protection Engineering Department resources, and therefore not included in the budget provided by the Chemical Engineering Department.